

# Synthesis of $\text{MnFe}_2\text{O}_4$ Nanoparticles as a Basic Material for Microwave Absorber

*Rika Rahmayanti<sup>1</sup> and Sudiati<sup>2\*</sup>*

<sup>1,2</sup>Department of Physics, Faculty of Mathematics and Natural Science, Universitas Sumatera Utara, Medan 20155, Indonesia

**Abstract.** This work aimed to synthesize  $\text{MnFe}_2\text{O}_4$  nanoparticles using the coprecipitation method. Manganese chloride dihydrate ( $\text{MnCl}_2 \cdot 4\text{H}_2\text{O}$ ) and iron sand from South Cianjur, Indonesia, were used as a precursor for  $\text{MnFe}_2\text{O}_4$  nanoparticle synthesis. The iron sand elements and compounds were tested using X-Ray Fluorescence (XRF).  $\text{MnFe}_2\text{O}_4$  nanoparticle was characterized using X-Ray Diffraction (XRD), Scanning Electron Microscope-Energy Dispersive X-Ray (SEM-EDX), and Vector Network Analyzer (VNA). The X-Ray Fluorescence test result showed that 70.54% of South Cianjur contained iron sand. The SEM test result showed that the nanoparticles have an average size of 73.75 nm with a round shape, which was attributed to the agglomeration process. The EDX test result showed that the synthesized nanoparticle contained only Mn, Fe, and O elements without contaminants. The XRD test result showed that the crystal phase of  $\text{MnFe}_2\text{O}_4$  was formed with a crystal size of less than 27 nm. The largest reflection losses in the 11.5 - 12.5 GHz range were found in  $\text{MnFe}_2\text{O}_4$  with 1:2 variation, i.e., 35.08 dB. This study found that adding iron sand increases  $\text{MnFe}_2\text{O}_4$  microwave absorption.

**Keywords:** Coprecipitation,  $\text{MnFe}_2\text{O}_4$ , Nanoparticles, Iron sand.

Received 22 December 2021 | Revised [15 August 2022] | Accepted [29 August 2022]

## 1 Introduction

Technology, especially electronic devices and wireless communications has exhibited significant advancement. Microwave technology also becomes increasingly popular and has found its use in household, industry, communication, medical application, and military sectors, generating spontaneous electromagnetic emissions into the atmosphere [1]. Cellular phones that work at high frequency is responsible for frequency leak that decreases electronic device performance [2]. In this regard, microwave absorbers are expected to provide an effective solution to control microwave impacts [3]. The application of iron sand and manganese should be within nanometers to support the development of nanomaterial study [4].

Indonesia possesses an abundant iron sand reserve [3]. The south coast of Java Island contains abundant ferum-producing minerals in gray and black color with soft textures [5]. Hence, the

---

\*Corresponding author at: Jalan Bioteknologi no.1 Medan, 20155, Indonesia

E-mail address: sudiati@usu.ac.id

iron sand utilization needs further development. Furthermore, the iron sand application in industrial and medical sectors would be more optimal if it is nano-sized [6]. Manganese ferrite ( $\text{MnFe}_2\text{O}_4$ ) is one of the materials with strong properties and an equilibrium external field effect [7]. Therefore, this study focuses on the synthesis of ( $\text{MnFe}_2\text{O}_4$ ) from the iron sand obtained on the south coast of Java Island.

Several methods and techniques for synthesizing magnetic nanoparticles include sol-gel, vapor condensation, microemulsion, combustion, and coprecipitation. The coprecipitation method was selected for its efficiency and applicability at room temperature, affordability, and simplicity. The coprecipitation method is also reported to generate more homogeneous particles than other methods [8]. The normal condition can also be applied to this method [9]. The disadvantage of this method lies in particle agglomeration due to its inability to control particle size [10]. Based on the earlier description, it is necessary to conduct a study on the synthesis of ( $\text{MnFe}_2\text{O}_4$ ) from iron sand on the South Coast of Java Island.

## 2 Materials and Methods

### 2.1 Materials

Materials used in this study include iron sand from the southern coast of Cianjur, Indonesia, a 99.9% pure manganese chloride powder produced by Merck, 37% chloride acid solution by Merck, Sodium hydroxide produced by Merck, and Ethanol 96% produced by Merck.

### 2.2 Manganese Ferrite Nanoparticle Synthesis

The first stage in this study was to sieve the iron sand sample using a 200 mesh sieve, followed by X-Ray Fluorescence (XRF) test. Then,  $\text{MnCl}_2 \cdot 4\text{H}_2\text{O}$  and South Cianjur iron sand were dissolved using 2M NaOH with concentration ratios of 1:1, 1:2, and 2:1 and stirred for two hours. After that, the sample was washed to obtain a neutral pH level and calcined for one hour at 800 °C before being tested and characterized.

## 3 Result and Discussion

### 3.1 X-Ray Fluorescence (XRF) Test

XRF test results showed that iron sand from South Cianjur contains many elements. The most dominant element was iron (Fe) (70.5%), followed by Ti, Mg, Si, Al, and other small elements (Table 1).

**Table 1.** Elements of South Cianjur Ironsand

Element	Fe	Ti	Mg	Si	Ag
Concentration (%)	70.548	10.537	6.985	4.389	1.728

### 3.2 X-Ray Diffraction (XRD) Analysis

Following the XRD characterization, the  $\text{MnFe}_2\text{O}_4$  nanoparticle sample was synthesized using the coprecipitation method (Figure 1). The diffraction peaks were well-defined at the angles of  $23.1^\circ, 31.6^\circ, 32.9^\circ, 49.5^\circ, 54.1^\circ, 55.2^\circ,$  and  $65.7^\circ$  with Miller indexes of (211), (222), (400), (411), (332), (134) (422), (440), (145), (311) and (531). In general, the  $\text{MnFe}_2\text{O}_4$  phase is formed in the fields (111), (220), (222), (400), (311), (422), (511), and (440) [4]. In this study,  $\text{MnFe}_2\text{O}_4$  was formed in fields (222), (400), (311), (422), and (400). Meanwhile, other peaks appear to emerge due to impurity.

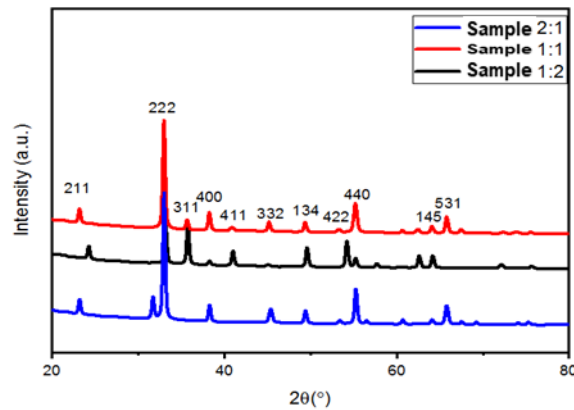


**Figure 1.** XRD pattern of  $\text{MnFe}_2\text{O}_4$  nanoparticle

As shown in Figure 2, different concentrations resulted in lattice shifts. Each sample had different intensities, and the highest intensity was found in the sample with a 2:1 concentration variation, followed by 1:1 and 1:2 concentration variations. This condition may occur as the increased Mn dope leads to higher intensity.

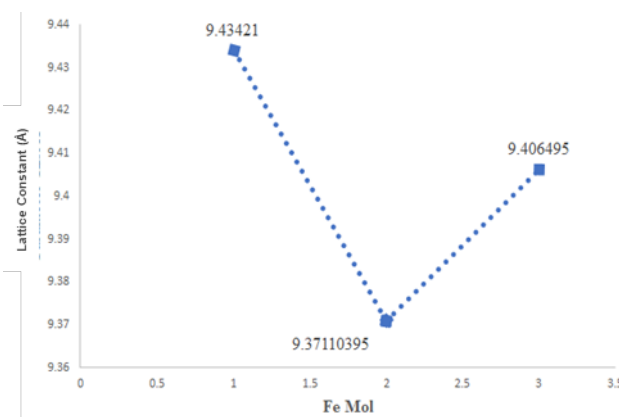


**Figure 2.** The Effect of Fe mole on lattice parameter Water Absorption

As shown in Figure 2, the XRD analysis showed that the sample with 1:1, 2:1, and 1:2 concentrations exhibited a lattice parameter of  $9.43421 \text{ \AA}$ ,  $9.406495 \text{ \AA}$ , and  $9.37110395 \text{ \AA}$ , respectively. Based on the cubic crystal structure of spinel  $\text{MnFe}_2\text{O}_4$ , the  $a=b=c$  value was  $0.94 \text{ nm}$  [11].

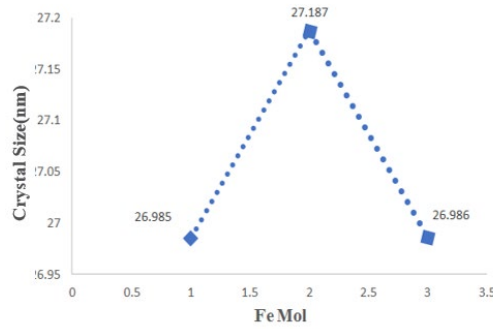


**Figure 3.** The Effect of Fe on crystal size

The crystallite size for samples 1:1, 1:2, and 2:1 was 26.985 nm, 27.187 nm, and 26.986 nm, respectively (See Figure 3). Therefore, several factors are expected, such as the combination of acid and base chemical compounds, which affect the pH level of the solution [12].

The lattice parameter value was inversely proportional to the crystal size, indicated by the lower lattice value as Fe was added and the crystal diameter increased. The crystal size was directly proportional to Fe addition, meaning that larger Fe composition leads to a larger crystal size. In other words, more Fe addition causes larger crystal diameters and lower lattice parameter values.

### 3.3 Scanning Electron Microscope-Energy Dispersive X-Ray (SEM-EDX) Analysis

The morphological structure analysis of a micro-structural material and particle size of Manganese Ferrite was made using an SEM test.

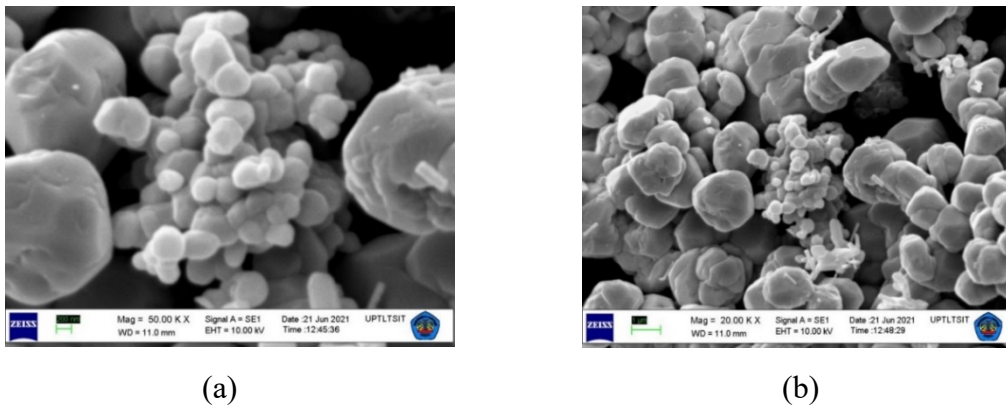


**Figure 4.** Morphology of 2:1  $\text{MnFe}_2\text{O}_4$  powder with 50,000 magnification (a) 2:1  $\text{MnFe}_2\text{O}_4$  with 20,000 magnification (b)

SEM analysis of 2:1  $\text{MnFe}_2\text{O}_4$  powder is given in Figure 4. Figure 4 also shows that the average particle size was 73.75 nm with a round shape (Figure 5). In Mai's (2020) study,  $\text{Fe}_2\text{O}_3$  showed a rod shape, while  $\text{Mn}_2\text{O}_3$  showed a round shape. This is related to the XRD result, which indicates a more dominant  $\text{Mn}_2\text{O}_3$  phase. On average,  $\text{Mn}_2\text{O}_3$  nanoparticle size was smaller than  $\text{Fe}_2\text{O}_3$ . The increase in nanoparticle size is often attributed to agglomeration [13].

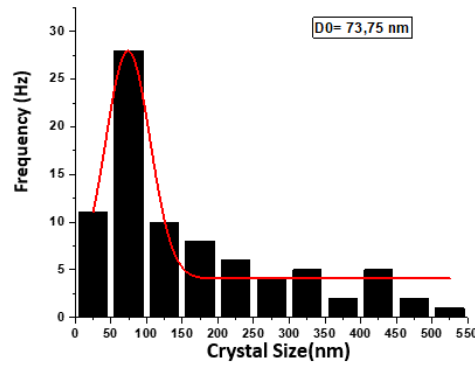


**Figure 5.** Histogram of particle size distribution

Table 2 displays the weight percent and atomic percent of the element  $\text{MnFe}_2\text{O}_4$ .

**Table 2.** Analysis of  $\text{MnFe}_2\text{O}_4$  element using SEM-EDX

<i>Element</i>	<i>Weight(%)</i>	<i>Atomic(%)</i>
Fe	37.4	21.90
Mn	34.42	20.49
O	28.18	57.60

As displayed in Table 2, Fe has a higher weight percentage (37.4 wt%) than Mn (34.42%) and O (28.185 wt%). Regarding atomic percentage, Fe has 21.90%, while Mn and O have 20.49% and 57.60%, respectively. The test in this study consists only of manganese, ferum, and oxygen. The presence of oxygen in high density could be attributed to the adsorption of water molecules [14].

### 3.4 Vector Network Analyzer (VNA)

Figure 6 showed that in 11.5-12.0 GHz frequency, the three samples exhibited the same pattern. The Red line represents a 1:1 concentration variation, while the black and blue lines represent 1:2 and 2:1 concentration variations, respectively.

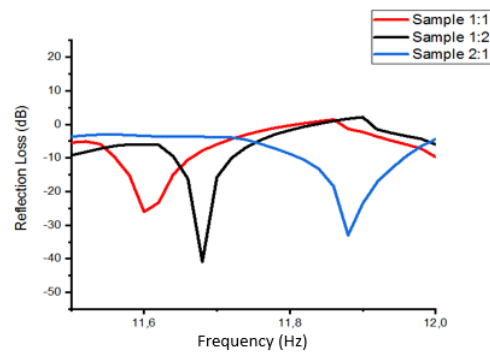


**Figure 6.** The reflection loss at 11.5-12.0 GHz

Reflection loss refers to the size of electromagnetic wave energy after imposing a material. A minimum reflection loss indicates good material absorption [15]. The valley indicates the presence of absorption, and the wide valley represents good absorption [16]. The reflection loss curve at 11.5 - 12.0 Hz showed that sample 1:2 has the lowest reflection loss (i.e., -35.08) at 11.68 Hz. This occurred because sample 1:2 contains more iron sand than manganese.

**Table 3.** MnFe<sub>2</sub>O<sub>4</sub> sample absorption

Sample name	Reflection Loss (dB)	Frequency (GHz)	Reflection coefficient ( $\Gamma$ )	Absorption (%)
1:1	-26.03	11.6	0.04994	95.00
1: 2	-35.08	11.68	0.00903	98.23
2: 1	-32.97	11.88	0.02246	97.75

As displayed in Table 3, sample 1:2 showed the highest reflection loss at 11.6-11.88 Hz (35.08 dB), while Samples 2:1 and 1:1 reflection loss was -32.97 dB and -26.03 dB, respectively.

Overall, the increase in material absorption is accounted for by Fe addition, as demonstrated in Table 3, in which sample 1:2 has a high absorption due to more phases (Fe<sub>2</sub>O<sub>3</sub>), eventually resulting in higher reflection loss. This occurs because Fe<sub>2</sub>O<sub>3</sub> has the antiferromagnetic property responsible for weaker magnet properties than single-phase composition [2]. Reflection loss indicates the absorption percentage. For example, a reflection loss of 10 dB means that the wave absorption may reach 90%, and a reflection loss of dB 20% indicates a 99% wave absorption [17]. The test result in this study showed that MnFe<sub>2</sub>O<sub>4</sub> showed a small absorption bandwidth yet a fairly good absorption ability.

#### 4 Conclusion

The present study synthesized MnFe<sub>2</sub>O<sub>4</sub> with 1:1, 1:2, and 2:1 concentration variations using the coprecipitation method. The XRD result showed that the MnFe<sub>2</sub>O<sub>4</sub> nanoparticles have a cubic crystal shape with lattice parameter  $a=b=c$ ,  $9,37 = 9,43 = 9,40\text{\AA}$ . The smallest crystallite size was found in sample variation 1:1 (26.985 nm). The lattice parameter and crystal diameter were inversely proportional to Fe addition. SEM characterization results showed that MnFe<sub>2</sub>O<sub>4</sub> formed 73.75 nm round nanoparticles. Fe addition resulted in the highest negative reflection loss in sample 1:2 (i.e., -35,08 dB). This study reported good electromagnetic wave absorption, as indicated by large absorption power yet low absorption bandwidth.

#### REFERENCES

- [1] Z. Jing, R. Qinghong, and Y. Atassi, "Design of ternary-Component X-Band Microwave Absorber Based on FeCo/Sr hexaferrite/PANI nanocomposite In Silicon Resin Matrix," *Journal of Magnetism and Magnetic Materials*, vol. 512, no. 167037, 2020.
- [2] Mashadi, R. A. Putri, B. Sugeng, and Yunasfi, "Sintesis Bahan magnetik Zn<sub>x</sub>Fe<sub>(3-X)</sub>O<sub>4</sub>

- dengan metode ko-presipitasi sebagai penyerap gelombang mikro," *Majalah Ilmiah Pengkajian Industri*, vol. 13, no. 2, pp. 179-186, 2019.
- [3] T. Oktafiana, "Analisis Fasa, Sifat Magnetik, Dan Penyerapan Gelombang Mikro Bahan Serbuk Magnetit ( $\text{Fe}_3\text{O}_4$ )-Semen Portland Tipe I," Undergraduate Thesis, Institut Teknologi Sepuluh Nopember, Surabaya, 2016.
- [4] Rajab, "Sintesis Nanopartikel Manganese Ferrite ( $\text{MnFe}_2\text{O}_4$ ) Berbasis Pasir Besi dan Mangan Alam dengan Metode Reaksi Padatan," Undergraduate Thesis, Universitas Haluoleo, Kendari, 2017.
- [5] D. Setiady, E. H. Sudjono, D. Z. Hans, and S. Sutardi, "Kandungan Mineral Pada Pasir Besi di Pantai Loji dan Ciletuh, Kabupaten Sukabumi, Jawa Barat Berdasarkan Data Bor Dan Georadar," *Jurnal Teknologi Mineral dan Batubara*, vol. 16, no. 3, pp. 125-138, 2020.
- [6] S. Nengsih, "Potensi nanopartikel magnetit pasir besi lampanah aceh besar melalui studi kajian teknik pengolahan, sintesis dan karakteristik struktur," *Circuit: Jurnal Ilmiah Pendidikan Teknik Elektro*, vol. 2, no. 1, 2018.
- [7] P. Nixcoriani, "Sintesis nanopartikel Manganese Ferrite ( $\text{MnFe}_2\text{O}_4$ ) dari pasir besi dan mangan alam dengan metode kopresipitas," *Jurnal Fisika Unand*, vol. 9, no. 3, 2020.
- [8] M. A. Yunasfi, and Nurhasni, "Sifat magnet dan serapan gelombang mikro  $\text{Mn}_{(1-x)}\text{Nd}_x\text{Fe}_2\text{O}_4$  hasil sintesis dengan metode ko-presipitasi," *Jurnal ILMU DASAR*, vol. 19, no. 1, pp. 17-22, 2018.
- [9] T. Ajeesha, A. Ashwini, M. George, A. Manikandan, J. A. Mary, Y. Slimani, and A. Baykal, "Nickel Substituted  $\text{MgFe}_2\text{O}_4$  Nanoparticles Via Coprecipitation Method for Photocatalytic Applications," *Physica B: Condensed Matter*, vol. 606, no. 412660, 2020.
- [10] A. N. Lisdawati, "Pengaruh variasi suhu dan waktu kalsinasi pada pembentukan fasa  $\text{ZrO}_2$ ," M.S. Thesis, Institut Teknologi Sepuluh Nopember, Surabaya, 2015.
- [11] Y. H. Son, P. Bui, H. R. Lee, M. S. Akhtar, D. K. Shah, and O. Yang, "A Rapid Synthesis Of Mesoporous  $\text{Mn}_2\text{O}_3$  Nanoparticles For Supercapacitor Applications," *Coatings*, vol. 9, no. 10, 2019.
- [12] V. Herika, "Sintesis  $\text{Mg}_{1-x}\text{Ni}_x\text{Fe}_2\text{O}_4$  Berbasis Pasir Besi Alam Sebagai Adsorben Ion Logam Berat," Undergraduate Thesis, Universitas Sumatera Utara, Medan, 2018.
- [13] Z. Cahyarani, "Pengaruh Penambahan Tetraethyl Orthosilicate (TEOS) Sebagai Material Coating Pada Nano Partikel  $\text{Fe}_3\text{O}_4$  Untuk Aplikasi Nano Lubricant," Undergraduate Thesis, Universitas Sumatera Utara, Medan, 2019.
- [14] Y. Ghaffari, N. K. Gupta, J. Bae, and K. S. Kim, "One-step Fabrication of  $\text{Fe}_2\text{O}_3/\text{Mn}_2\text{O}_3$  Nanocomposite for Rapid Photodegradation of Organic Dyes at Neutral pH," *Journal of Molecular Liquids*, vol. 315, no. 113691, 2020.
- [15] N. Awaln, "Studi penyerapan gelombang elektromagnetik rentang X-Band dengan menggunakan penyerap PANi konduktif dan barium M-Heksaferrit terdoping ion Zn ( $0,3 \leq X \leq 0,9$ )," Undergraduate Thesis, Institut Teknologi Sepuluh Nopember, Surabaya, 2017.
- [16] D. Andriyani, "Karakterisasi perilaku radar absorbansi material (RAM) berbasis BAM & PANI dengan struktur geometri multilayer untuk rentang penyerapan X-Band," Undergraduate Thesis, Institut Teknologi Sepuluh Nopember, Surabaya, 2018.
- [17] S. Wardiyati, W. A. Adi, and D. S. Winatapura, "Sintesis dan karakterisasi microwave absorbing material berbasis Ni-SiO<sub>2</sub> dengan metode sol-gel," *Jurnal Fisika*, vol. 8, no. 2, pp. 51-59, 2018.